Development of a Nonlinear K-Law Spectral Signature Index to Classify Basophilic Inclusion Bodies of the White Spot Syndrome Virus

Mario Alonso Bueno Ibarra
María Cristina Chávez Sánchez
Laboratorio de Histología
Centro de Investigación en Alimentación y Desarrollo A.C. (CIAD)
Av. Sábalo-Cerritos S/N, Estero del Yugo.
Mazatlán, Sinaloa, México, C.P. 82000
mbueno@digitalsoftsystems.com
marcris@ciad.mx

Josué Álvarez-Borrego
División de Física Aplicada, Departamento de Óptica.
Centro de Investigación Científica y de Educación Superior de Ensenada (CICESE)
Km 107 Carretera Ensenada-Tijuana No. 3918,
Fraccionamiento Zona Playitas.
Ensenada, Baja California, México, C.P. 22860.
josue@cicese.mx

***Abstract*—In this paper a novel technique is developed to classify White Spot Syndrome Virus (WSSV) inclusion bodies found in shrimp tissues by the analysis of digitalized images from infected samples. Since the early 90's, WSSV has been affecting the economy of shrimp producers around the world restraining aquaculture production. Once the clinical signs are developed; mortality can reach 100% in 3 days. Several techniques have been implemented and developed for viral and bacterial diagnostics from penaeid shrimps; however histology is still considered the common tool in medical and veterinary diagnostics tasks. WSSV slide images were acquired by a computational image capture system and a new spectral signature index is developed to obtain a quantitative measurement of the complexity pattern found in WSSV inclusion bodies. Representative groups of WSSV inclusion bodies from infected shrimp tissues and organs were analyzed. The results show that inclusion bodies analyzed are well defined in a clear numerical fringe, obtained by the calculation by this spectral signature index.**

Keywords-WSSV; image processing techniques; inclusion bodies; shrimp; virus

I. INTRODUCTION

White Spot Syndrome (WSSV) is a highly contagious viral disease of penaeid prawns (Penaeidae family), characterized by rapid onset of high levels of mortality in farmed populations. However, all decapod crustaceans including prawns, lobsters and crabs from marine, brackish water or fresh water are considered susceptible to the infection [1]. Since 1992 to date, WSSV has been affecting the economy of shrimp producers around the world restraining aquaculture production [1].

WSSV can spread and infect shrimps of any stage of grow-out, asymptomatically affecting all life cycle stages, from eggs to broodstock. Once the clinical signs are developed, mortality can reach 100% in 3 days [1][2]. The causative agent of the disease is an ovoid or ellipsoid to bacilliform in shape double-stranded DNA virus (120-150 nm in diameter and 270-290 nm in length), which genus is Whispovirus, within the family Nimaviridae [1].

Several techniques have been implemented and developed for viral and bacterial penaeid shrimps diagnostics; these can be divided in traditional morphological pathology, bioassay, microbiology and serology and molecular methods such as PCR [3], however histology is still considered the common tool in medical and veterinary for research and diagnostics tasks [4].

Histology makes possible to analyze pathological changes in several tissue cells and allow the pathogen identification which are sometimes difficult to recognize with other alternative techniques. For this kind of analysis the method involves several steps to obtain the final sample, which contains a shrimp tissue slice where the inspection is conduced; this tissue slice has a thickness of 1-5 µm, stained with hematoxilin - eosin necessarily to make the examination under microscope [3][4][5].

WSSV infection is commonly seen in cuticular epithelial cells and connective tissue cells of the stomach, carapace and gills. However it is also seen in antennal gland, lymphoid organ, hematopoietic tissue and phagocytes of the heart. Infected cells typically have hypertrophied (enlarged) nuclei containing a single intranuclear inclusion. Inclusions at the beginning are eosinophilic and sometimes are separated by a clear halo beneath the nuclear membrane; these are known as Cowdry type A inclusions. Later inclusions become lightly to deeply basophilic and fill the entire nucleus [3][6], as shown in Figure 1.

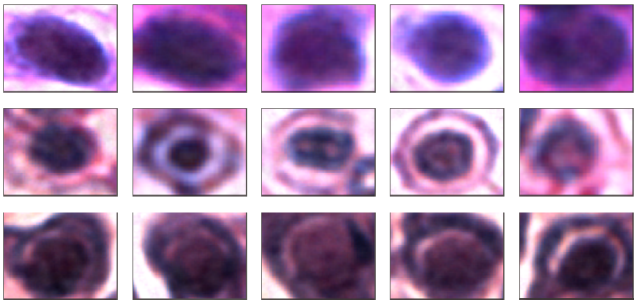

Figure 1. WSSV basophilic and Cowdry A type inclusion bodies.

978-0-7695-3968-3/10 $26.00 © 2010 IEEE
DOI 10.1109/BioSciencesWorld.2010.12

The need for rapid, sensitive diagnostic methods led to develop new alternative techniques in different fields of knowledge like computing optic disciplines that can be of support to conventional methods.

Several optic and computational techniques were developed to recognize these kinds of biological patterns, the analysis of inclusion bodies is determinant of the virus presence, thus color correlation approach was used to analyze and recognize the presence of IHHNV inclusion bodies by histological samples from 35 mm transparencies digitalized with a flatbed scanner [7].

The aim of this paper is to develop a new technique to classify the WSSV basophilic and Cowdry type A inclusion bodies, acquired from histological digitalized images from infected shrimps samples; afterwards an analysis is applied over these slide samples, based in the use of Fourier spectral filtering techniques, such as K-Law nonlinear filter.

In section II we describe the core basis of the methodology and the equipment used to obtain the images from infected shrimp tissues; in section III we present the results obtained with the spectral signature index developed; additionally the statistical analytic values obtained from this index and the experiments carried out from the digitalized images previously acquired are included; finally in section IV the possible future work that needs to be done to enrich this research is discussed.

II. MATHERIALS AND METHODS

Development of a new technique to classify WSSV inclusion bodies; subsection A describes how the shrimp samples were prepared; subsection B describes the equipment used for image capturing; subsection C explains the mathematical basis used for this technique; finally subsection D describes the steps involved in the obtaining of the classification by the signature index proposed.

A. Virus sample preparation

Experimental shrimps were obtained from a farm located in the state of Sinaloa, México; transported live to the laboratory to be fixed in Davidson's solution; after 24 h, the fixative was discarded and shrimps were preserved in 50% alcohol solution until they were ready to be processed by conventional histology techniques [3][4].

Once histological slides were ready to be examined under microscope, different types of inclusion bodies were selected from cuticular epithelium, connective tissue and abdomen tissue and were digitalized to obtain a bank of images.

B. Digitalized images capture

The WSSV slide images were acquired by a computational image capture system prototype to enhance the digitalized images with novel autofocus and fusion techniques developed [8][9], running inside a 2.5 GHz PC Pentium 4 with 1 GByte RAM and 80 GBytes HD attached to Leica microscope (model DMRXA2) equipped with a RGB color digital camera (Leica model DC300). A set of 168 microscope images were acquired from the shrimp's tissues by 60x objetive with a 2088 x 1550 pixels color resolution digital camera; each representative field can contains about an average of 30 to 60 approximately inclusion bodies depending of the level of WSSV infection. Afterwards, a set of 870 WSSV inclusion body images were selected to build a filter bank with 100 most representative WSSV images obtaining the intensity spatial domain matrix data of each WSSV image to be analyzed; thus multispectral function $f^{\lambda}(x,y)$ is defined for every pixel coordinates x an y on digitalized images, where $\lambda=\{\lambda_R,\lambda_G,\lambda_B\}$ acquired by a CCD's digital camera with range $[0,255]$ and red (R), green (G) and blue (B) are channels in RGB color space representation.

C. WSSV spectral signature index classifier

Let us introduce some useful definitions and functions: $f_1^{\lambda},f_2^{\lambda},f_3^{\lambda},...,f_w^{\lambda}$ are a multispectral filter bank of W captured images of size $N\times P$ pixels from inclusion body samples taken; $f_w^{\lambda}(x,y)$ is the captured image matrix with pixels (x,y) in the w^{th} inside filter bank images, where $x=1,...,P$, $y=1,...,N$ and $w=1,...,W$.

Spectral signature SSF can be defined like a function to obtain the spectral properties of $f_w^{\lambda}(x,y)$ from a specific RGB channels $\{\lambda_R,\lambda_G,\lambda_B\}$; whereas spectral signature index i^{ss} was developed to get a quantitative measurement of the inclusion bodies complexity pattern. Let i^{ss} be defined like scalar number valued $i^{ss}\in\Re^{+}$ to measure the spectral frequency properties found in $f_w^{\lambda}(x,y)$ obtained by SSF function. Let $I^{\lambda_G}(x,y)$ be the intensity matrix data obtained by $f_w^{\lambda}(x,y)$, where inclusion bodies characteristics are protruded and $I_{IB}^{\lambda_G}(x,y)$ is the intensity matrix data resulted after the application of the $I_{Mask}^{\lambda_G}(x,y)$ circular binary mask function over the area where the inclusion bodies are analyzed; thus $I_{IB}^{\lambda_G}(x,y)=I^{\lambda_G}(x,y)\vartriangle I_{Mask}^{\lambda_G}(x,y)$, where $\vartriangle$ represents the bitwise multiplication.

Let us A_{Mask} be defined such as the circular binary mask's total area over the region of interest analyzed of the inclusion bodies, defined by

$$A_{Mask}=\sum_{x,y} I_{Mask}^{\lambda_G}(x,y),\ for\ I_{Mask}^{\lambda_G}(x,y)>0. \qquad (1)$$

K-Law nonlinear filter function (K-Law) in pattern recognition is used to analyze and explore the discriminating property quality of each filter [10] over the inclusion bodies segmented image $I_{IB}^{\lambda_G}(x,y)$ function.

K-Law filter function is derived by the Fourier transform of the $I_{IB}^{\lambda_G}(x,y)$ function, denoted by

$$I_{IB}^{\lambda_G}(u,v) = \left| I_{IB}^{\lambda_G}(u,v) \right|^k \exp\left[-i\phi(u,v) \right],\ k = 1. \qquad (2)$$

The K-Law nonlinear filter of $I_{IB}^{\lambda_G}(x,y)$ is applied by the change of value $0 < k < 1$ in (2), where k is the nonlinear strength; thus intermediate values of k permit the variability of filter features [11].

Let $f_w^{\lambda_G}(u,v)$ function be defined by the application of K-Law Fourier related filter, calculated over the $I_{IB}^{\lambda_G}(x,y)$ denoted by

$$f_w^{\lambda_G}(u,v)_k = I_{K-Law}^{\lambda_G}(u,v)_w, \quad 0 < k < 1 \qquad (3)$$

where $k = 0.1$ is used in (2) and u,v are variables in frequency domain. The SSF function can be obtained by

$$SSF\left(f_w^{\lambda_G}(u,v)_k \right) = \begin{cases} 1, & if\ \mathrm{Re}\left(f_w^{\lambda_G}(u,v)_k \right) > 0 \\ 0, & otherwise \end{cases}, \qquad (4)$$

where $f_w^{\lambda_G}(u,v)_k$ is obtained by (3).

Finally, the spectral signature index i^{ss} is developed and can be defined by

$$i^{ss} = \left\{ \frac{SSF\left(f_w^{\lambda_G}(u,v)_k \right)}{\left(A_{Mask} \right)_w} \middle| (u,v) \in \mathbb{C} \right\}, \qquad (5)$$

where SSF and A_{Mask} are obtained respectively according by (4) and (1) for every image $f_w^{\lambda}(x,y)$ found in the inclusion bodies filter bank.

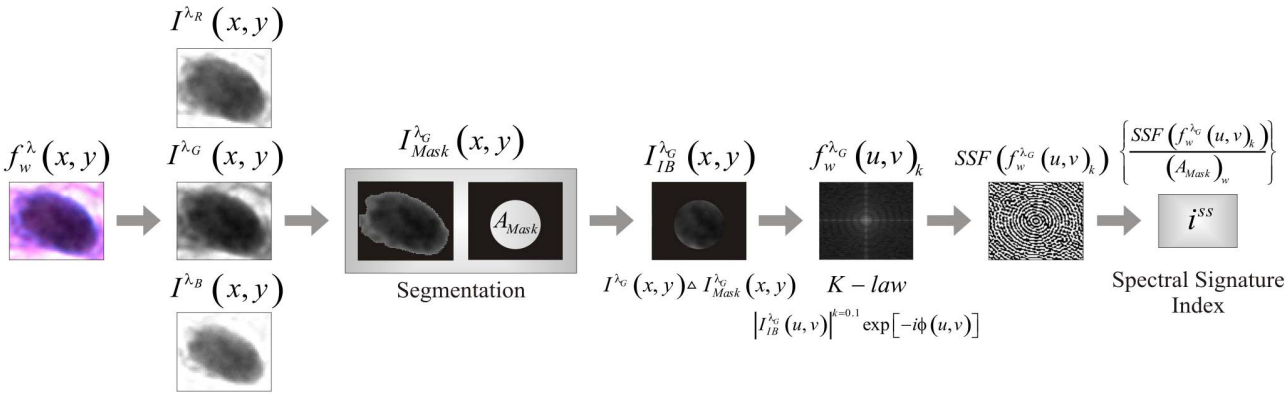

Figure 2. Block diagram to obtain the developed spectral signature index.

D. Spectral signature index classifier block diagram

Figure 2 shows the block diagram of the developed technique involved in inclusion bodies classification by the spectral signature index i^{ss}.

This methodology is explained by the following steps: 1) The $f_w^{\lambda}(x,y)$ function is acquired from WSSV inclusion bodies color image sample filter bank; 2) This $f_w^{\lambda}(x,y)$ is divided into its RGB $I^{\lambda_R}(x,y)$, $I^{\lambda_G}(x,y)$ and $I^{\lambda_B}(x,y)$ functions; 3) Using $I_{Mask}^{\lambda_G}(x,y)$ function, segmentation operation is applied over $I^{\lambda_G}(x,y)$ inclusion body area, where is obtained the $I_{IB}^{\lambda_G}(x,y)$ function; 4) The A_{Mask} variable is calculated from the $I_{Mask}^{\lambda_G}(x,y)$ binary mask function; 5) K-Law nonlinear operation is applied in $I_{IB}^{\lambda_G}(x,y)$ function to get the $I_{K-Law}^{\lambda_G}(u,v)_w$ function then it becomes into $f_w^{\lambda_G}(u,v)_k$ function in frequency domain; 6) The frequencies are extracted and analyzed from $f_w^{\lambda_G}(u,v)_k$ by the SSF and K-Law spectral signature index i^{ss} is calculated using (5).

III. RESULTS

In order to see if this technique is working with a good performance with the groups of representative inclusion bodies of WSSV with different morphological images, were analyzed with spectral signature index; their images and an additional group of non-infected tissue particles are shown in Figure 3; hence in Table 1 the statistical behavior values of the spectral signature index are shown, including the mean value $\pm 2SE$ (two standard errors).

A set of 168 microscope image field samples were acquired without any additional preprocessing like illumination or contrast correction just the fusion technique developed by [9]; then from this set 870 WSSV inclusion body images were cut, selecting 100 most representative WSSV inclusion bodies to build a filter bank from where the classification is calculated.

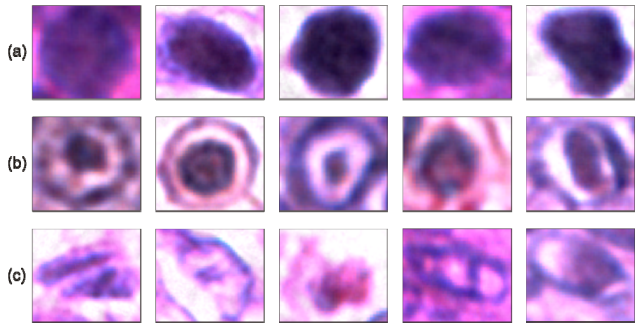

Figure 3. (a) WSSV strong basophilic inclusion bodies, group I; (b) WSSV white halo and chromatin Cowdry type A inclusion bodies, group II; (c) Non-infected tissue particles, group III.

TABLE I. SPECTRAL SIGNATURE INDEX STATISTICAL VALUES

WSSV Group	Signature Index Statistical Behavior			
	$\bar{x}_{i^{ss}}$	$\sigma_{i^{ss}}$	$1SE$	$2SE$
I	1.3748	0.4817	0.0852	0.1703
II	2.6069	1.8533	0.4953	0.9906
III[a]	159.4229	352.5394	94.2201	188.4402
IV[b]	1.7498	1.2362	0.1823	0.3645

a. Non-infected tissue group particles;
b. Groups I and II analyzed together.

The great difference in the statistical values of the infected particles with the non infected particles is due to the behavior of WSSV inclusion bodies frequencies in the green channel complex plane, while the non-infected cells do not show similar frequency properties; in Figure 4 are presented some examples of these frequencies behavior.

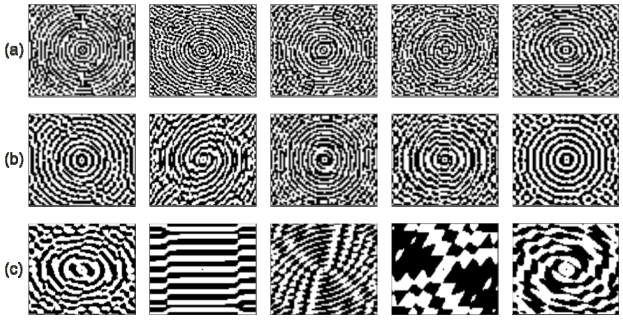

Figure 4. (a) SSF frequencies of group I; (b) SSF frequencies of group II; (c) Non-infected particles SSF frequencies, group III.

All the WSSV inclusion bodies were analyzed together; the results shows that the complete inclusion bodies group can be located in well defined fringe $1.3853 \le i^{ss} \le 2.1143$ with $(\pm 2ES)$.

IV. CONCLUSION AND FUTURE WORK

This paper presents a new technique to classify WSSV inclusion bodies from infected shrimp tissue image, based on the analysis of frequencies found in the green channel with K-Law non-lineal filter.

Representative groups of WSSV inclusion bodies from infected shrimp tissues and organs were analyzed. The results show that inclusion bodies are well defined in a clear numerical fringe; thus it can be inferred that whatever analyzed particle with a spectral signature index i_k^{ss} value outside of $1.3853 \le i^{ss} \le 2.1143$ range can be considered as non-infected particle.

Future work can be done in the development of automatic WSSV identification system applying this spectral index classifier; however this kind of classifier can be extended by combining complementary frequency analysis techniques by Fourier related filters on the calculation of the spectral signature index to obtain better discriminating results.

Experiments with new tissue samples can be done from others shrimps organs where the virus has a different pattern and its identification is more complex.

Finally, the potential of this signature index can be used to classify other kind of shrimp's viruses and/or other animal or human viruses.

ACKNOWLEDGMENT

This document is based on work partially supported by CONACYT under Grant No. 102007.

REFERENCES

[1] OIE, 2009. Manual of diagnostic test for aquatic animals. http://www.oie.int/eng/normes/fmanual/A_summry.htm

[2] Peinado-Guevara L. I. and López-Meyer M., "Detailed monitoring of white syndrome virus (WSSV) in shrimp commercial ponds in Sinaloa, México by nested PCR", Aquaculture, vol. 251, pp. 33–45, Issue 1, January 2006.

[3] Lightner D. V., "A Handbook on Shrimp Pathology and Diagnostic Procedures for Diseases of Cultured Penaeid Shrimp", World Aquaculture Society, Baton Rouge, LA, USA, 1996.

[4] Lightner D. V. and Redman R. M., "Shrimp diseases and current diagnostic methods", Aquaculture, vol. 164, pp. 201–220, Issue 1-4, May 1998.

[5] Bell T. A. and Lightner D. V., "A Handbook of Normal Shrimp Histology Special Publication No. 1", World Aquaculture Society, pp. 1–114, Baton Rouge, LA, USA, 1988.

[6] OIE, 2003. Manual of diagsnostic test for Aquatic Animals. http://www.oie.int/esp/normes/fmanual/A_summry.htm

[7] Álvarez-Borrego J. and Chávez-Sánchez M. C., "Detection of IHHN virus in shrimp tissue by digital color correlation" Aquaculture, vol. 194, Issue 1-9, August 2000.

[8] Bueno-Ibarra M. A., Álvarez-Borrego J., Acho L. and Chávez-Sánchez M. C., "Fast autofocus algorithm for automated microscopes", Optical Engineering, vol. 44(6), 063601-1, June 2005.

[9] Bueno-Ibarra M. A., Álvarez-Borrego J., Acho L. and Chávez-Sánchez M. C., "Polychromatic image fusion algorithm and fusion metric for automatized microscopes", Optical Engineering, vol. 44(9), 093201-1, September 2005.

[10] González-Fraga J.A., Kober V. and Álvarez-Borrego J., "Adaptive SDF filters for pattern recognition", Optical Engineering, Vol. 45, 057005, 2006.

[11] Guerreo-Moreno R. E. and Álvarez-Borrego J., "Nonlinear composite filter performance", Optical Engineering, vol. 48(6), 067201-1, June 2009.